A Mesoscale Analysis of Southern Plains Severe Convection on May 9, 2006

Michael Hiley
AOS453 - Professor Tripoli and Dan Henz
May 5, 2009

ABSTRACT

Two groups of severe convection in Oklahoma and Texas on May 9, 2006 are analyzed from the perspective of various data sources. The environment surrounding a group of discrete, supercellular convection in the Texas panhandle is contrasted with the one surrounding more linear convection in eastern Oklahoma. In both cases, forcing for convective initiation is found to be dominated by mesoscale boundaries in a region of relatively weak synoptic ascent; however, significant mesoscale differences between eastern Oklahoma and the Texas panhandle explain the majority of the observed differences in storm behavior in each area. Radar data demonstrates the importance of convective mode in determining type of severe weather produced, with discrete supercells favoring hail and tornadoes while the linear convection produces primarily high wind. Finally, a high resolution simulation of the event is performed with the Weather Research and Forecasting (WRF) model. The results of this model run are first compared to observations before being used to aid in diagnosing the event.

I. Introduction

On May 9, 2006 a round of intense storms impacted the Texas panhandle and eastern Oklahoma, leading to several tornado reports, including one tornado ranked as a three on the Fujita scale, which caused three fatalities in Westminster, Texas (NWS Ft. Worth), as well as about four significant (greater than 2") hail reports. As the storms in eastern Oklahoma organized and moved into Arkansas overnight on May 10, scattered damaging wind gusts (greater than 50 knots) were reported across much of the western half of the state (Fig. 1).

In terms of the areal coverage, quantity, and power of the severe weather produced, this event barely compares to many of the more infamous Great Plains severe weather outbreaks of early May. As just one example, the outbreak of May 4-5, 2007 produced over 80 tornado reports in states from Oklahoma all the way to Iowa and South Dakota, including the first tornado to receive a rating of five on the Enhanced Fujita scale in Greensburg, Kansas on May 4, 2007, which killed at least 11 people.

However, the three fatalities in Westminster on May 9, 2006 demonstrate that even events which may seem minor when compared to classic outbreak type events can and do produce powerful and destructive weather. As a result, it is important to understand and study more subtle events like the subject of this paper. While massive outbreaks like May 4-5, 2007 tend to be synoptically evident with many clues to warn of the coming significant weather, events like this one are far more subtle; the process of finding the mechanisms that will eventually result in convective initiation can actually be more complex, and the clues leading to a successful forecast can require a far more mesoscale-minded analysis of the data.

Consequently, this paper will attempt to characterize and analyze the mesoscale environments that led to the two primary areas of severe weather on May 9, 2006: the Texas panhandle and the eastern half of Oklahoma. While the two areas are only separated by about 200 km, the character of the resulting storms was quite distinct.

In the Texas panhandle, initiation occurred along a north-south line around 23Z, resulting in a line of discrete supercells. The cells exhibited splitting behavior and tended to remain quite discrete. These storms produced primarily very large hail, with about three reports of 2-2.5" hail and a single report of 4.5" hail in Samnorwood, Texas. Later in the evening, one storm became tornadic, producing an F2 tornado on the east side of Childress, Texas (NWS Lubbock).

In eastern Oklahoma, initiation also occurred around 23Z, however, the evolution of these storms was quite different from those in the Texas panhandle. The initial

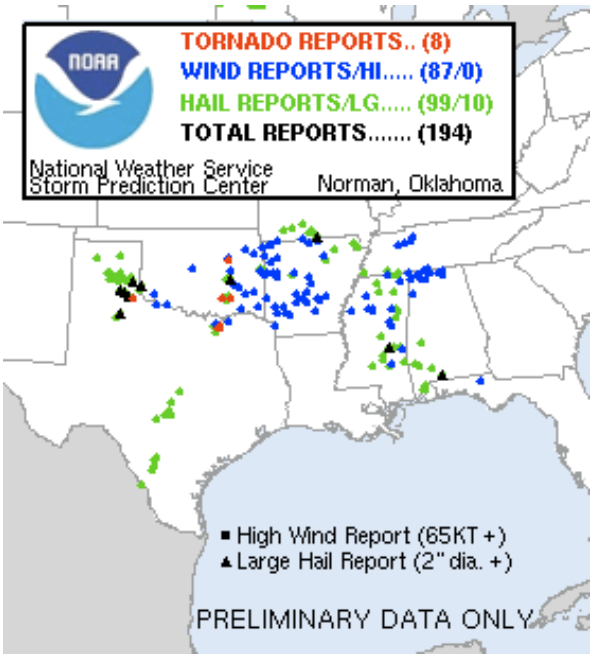

Fig. 1: SPC storm reports for May 9, 2006.

convection was indeed cellular and produced two brief tornadoes, but by 00:30Z the storms had already begun congealing into a single line. By 2Z on May 10, a single line of convection had become established in extreme southeast Oklahoma, producing primarily severe winds. However, a single discrete cell roughly 75 km south of the southern end of the line produced the F3 tornado in Westminster, Texas.

Gallus et al. (2008) statistically demonstrates the importance of convective mode in determining the type and intensity of severe weather produced: lines of discrete, cellular storms tend to produce primarily hail and tornadoes, while squall lines and bow echoes have severe wind as the greatest threat. The two groups of storms in the current case are generally consistent with these findings. The line of discrete cells in Texas produced large hail and one significant tornado. The more congealed, linear convection in Oklahoma produced primarily wind, with a single discrete cell at the south end of the line producing a significant tornado.

Despite the importance of storm mode in determining the type of severe weather produced, short-term prediction of storm mode remains a difficult problem in the operational forecast environment (Dial and Racy 2004). This provides the primary motivation for this paper: to investigate the reasons for such distinct storm modes by comparing and contrasting the mesoscale environments in which each group of storms formed. Focus will be placed the evolution and character of initiating boundaries as well as vertical shear profiles. It will be shown how extreme mesoscale variability led to the two distinct storm environments, and that through careful diagnosis of these

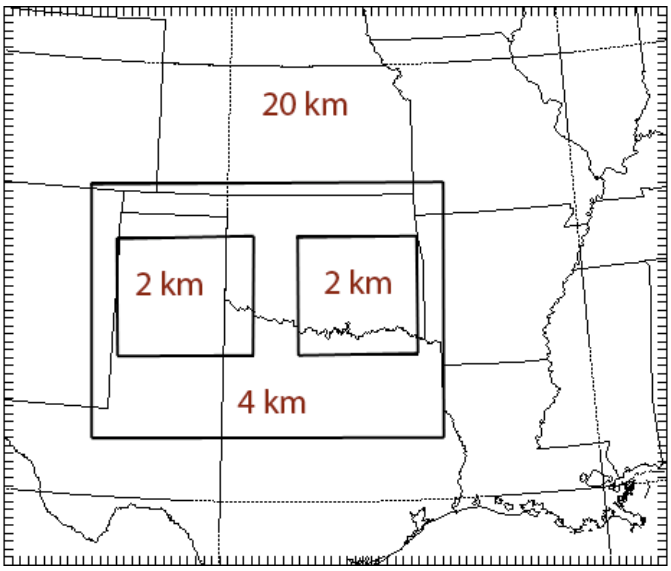

Fig. 2: Domain configuration of WRF simulation. Each domain is labelled with its corresponding resolution.

environments, many of the characteristics of the two groups of storms can be explained.

In addition, a high resolution run of the Weather Research and Forecasting (WRF) model is used. While the primary purpose of using the WRF model will be to aid in investigating mesoscale details of this event, it should be noted that high resolution models that simulate convection explicitly (i.e., without parameterization) are coming into increasing use in the operational forecast environment (Kain et al. 2006), and thus some evaluation of the ability of the WRF model to simulate this event will be performed in order to gain insight into its utility in forecasting severe storms.

II. Data

In order to investigate this event, various data sources were used. Level II radar data was obtained from the National Climatic Data Center archive. GOES-12 satellite data was obtained from the geostationary satellite archive at the Space Science and Engineering Center at the University of Wisconsin-Madison.

4-panel plots from the online image archive at Unisys Weather were used to assess the synoptic environment. Operational Eta model runs from May 9, 2006 at 12Z and May 10, 2006 at 00Z as well as observed surface and upper air data were also used.

Information regarding Storm Prediction Center (SPC) outlooks and mesoscale discussions was obtained from the SPC's online event archive. In addition, any storm reports not otherwise referenced were obtained from this source.

The Advanced Research WRF (ARW) modeling system (Skamarock et al. 2005) was used to perform a high resolution simulation of the May 9, 2006 event in order to better investigate mesoscale details. Six-hourly operational Eta model analyses on a 40 km grid (data set DS609.2, available from the CISL Research Data Archive at http://dss.ucar.edu/) from this date were used to provide initial and boundary conditions for the WRF.

Several model runs were performed using various domain configurations, but the most reasonable results were obtained using a four domain configuration (Fig. 2), and therefore is the only WRF run discussed from this point on. The coarsest grid used a 20 km resolution and extended in the north-south direction from southern Texas to southern Nebraska, and western Colorado to western Kentucky in the east-west direction. A second domain with 4 km resolution was nested inside this, covering the entire state of Oklahoma and the northern half of Texas. Finally, two separate 2 km resolution grids were nested inside of the 4 km grid, the first covering the Texas panhandle and the second covering the eastern half of Oklahoma, in order to provide the best simulation of the regions of primary interest.

The model was initialized at 12Z on May 9, 2006 and run for 18 hours, requiring about 24 hours of processing time on a modest 2007-era AMD processor. The majority of the details of the model setup will be forgone except for one important note: Weisman et al. (2008) suggests that a 4 km resolution is sufficient to simulate convection without parameterization. Thus convective parameterization was turned off for the 4 km and 2 km grids.

The McIDAS-V application was used to produce radar and satellite plots. Vis5D was used to visualize WRF model output. Finally, the GEMPAK software package was also used to analyze WRF output, as well as to create surface, observed upper-air, and Eta model plots.

III. Synoptic Overview

First, the event will be described from a synoptic perspective, with a focus on large-scale forcing mechanisms and other necessary severe weather ingredients such as moisture sources and steep mid-level lapse rates.

Beginning with the 12Z situation (Fig. 3), the most striking feature is a long, north-south oriented pressure trough evident at the surface and 850 mb. This low pressure area resulted in a large area of convergence, as evidenced by a surface wind-shift line from Minnesota to the Texas panhandle, with generally 5-10 knot northwesterly flow on the northwest side of the front and 5-10 knot southeasterly flow on the east side of the front. The morning 12Z Hydrometeorological Prediction Center (HPC) surface analysis depicted a cold front through this convergence zone, however the temperature contrast between the two air masses was fairly small, with surface temperatures generally in the mid-40's (F) on

the west side of the front and mid-50's on the east side. However this front contributed to the later evolution of the setup in one important way: by supporting a prefrontal band of storms from northeast Oklahoma to southeast Iowa. This helped reinforce a separate surface boundary stretching east-west across Oklahoma by bringing rain-cooled air to the surface on in northern Oklahoma and therefore increasing the temperature contrast across the east-west front. This frontal zone extended eastward from a weak surface low in western Oklahoma, and would become important as a mechanism to help focus surface convergence and therefore initiate convection later in the day.

At 850 mb, the surface low in Oklahoma was reflected as a geopotential height minimum near the same location. Note the strong west-southwesterly flow to the south of this low, advecting very warm air and thereby contributing to a strong capping inversion centered at this level over Texas and Oklahoma. This served to keep the warm sector capped through the morning and allow surface heating to increase convective available potential energy (CAPE) values throughout the day, allowing storms to reach maximum intensity by the time initiation finally occurred later in the afternoon. Paired with the very warm 850 mb air was a strong elevated mixed layer (EML) above, with nearly dry-adiabatic lapse rates in the 850-500 mb layer evident in 12Z soundings

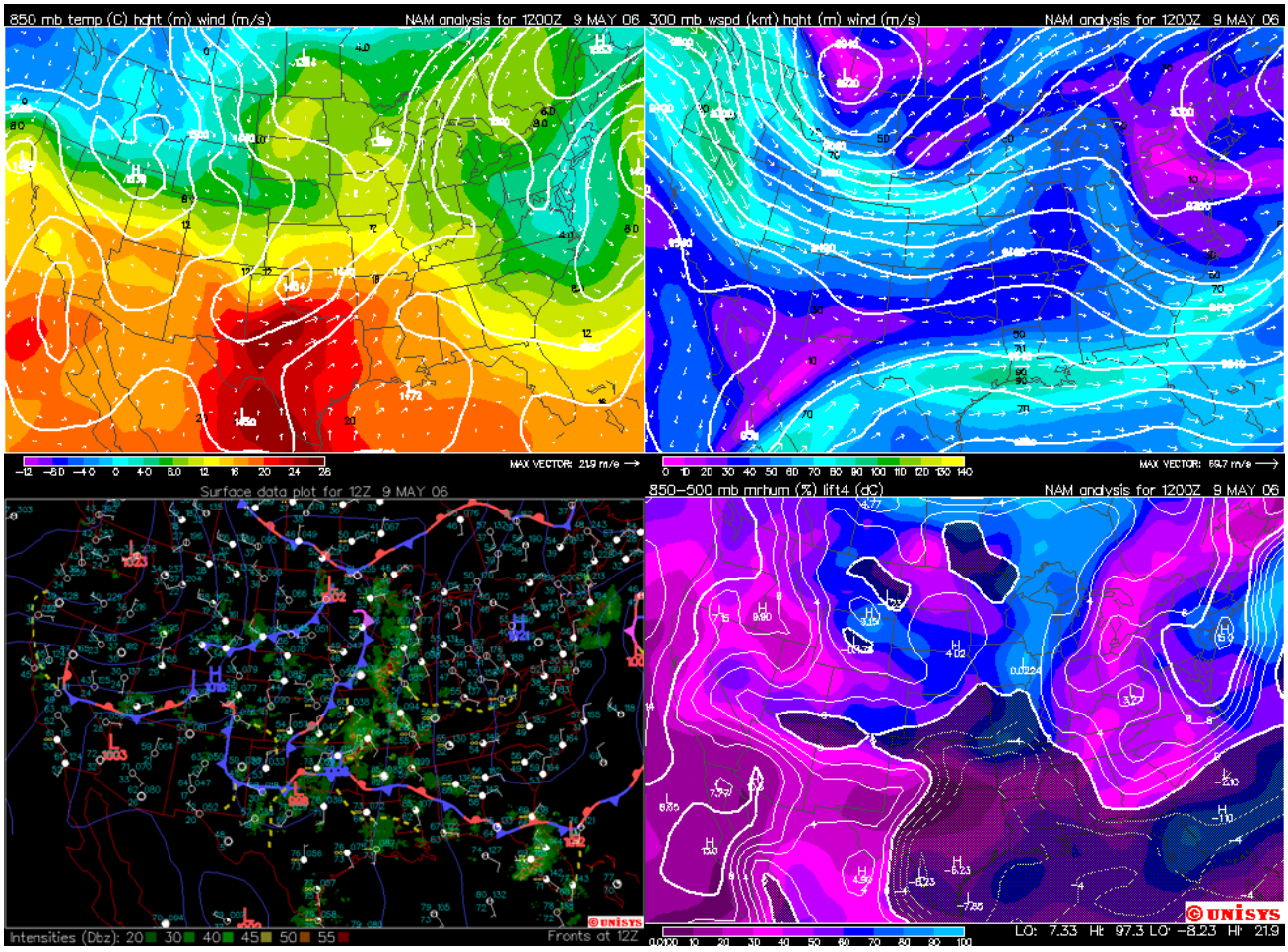

Fig. 3: Four-panel plot from Unisys Weather showing the synoptic situation at 12Z on May 9, 2006. The parameters are labelled on each plot.

across most of Oklahoma and northern Texas.

In addition, surface dewpoints were already in the low-70's (F) to the south of the front in Oklahoma. Combined with the steep mid-level lapse rates described above, the result was a convectively unstable but capped air mass, as evidenced by lifted indices already in the -6C range across eastern Texas and the southeast portion of Oklahoma by 12Z. With the addition of surface heating throughout the coming day, the air mass would become extremely unstable by afternoon, with surface-based CAPE values above 5000 J/kg by late afternoon.

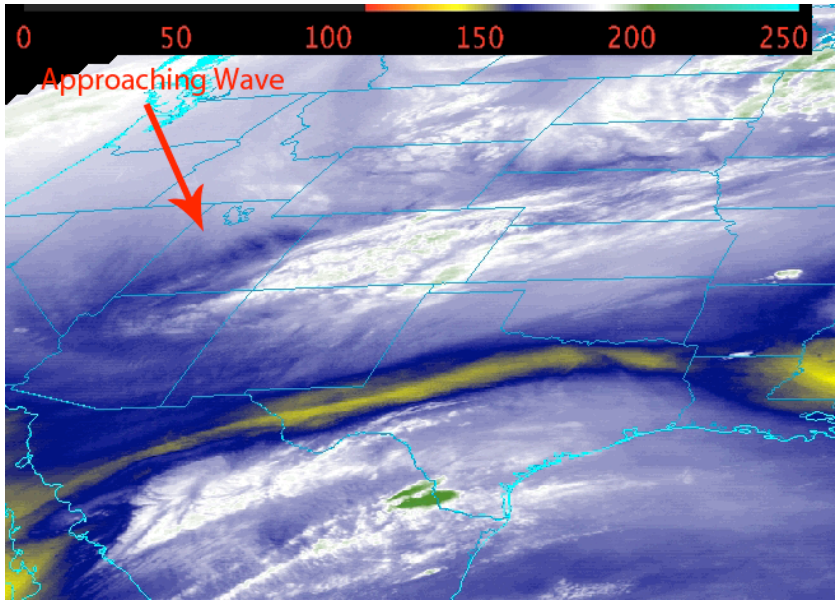

Fig 4: 4 km resolution GOES12 Water Vapor Channel (6.5μm) Imagery from 21:15Z on May 9, 2006.

The synoptic upper-air pattern also appeared to be supportive of the possibility of severe weather later in the day. At 300 mb, a broad trough was evident with approximately 70 m/s (135 knot) flow from Idaho through Wyoming and Nebraska. However, simple flow curvature arguments would lead one to believe the primary rising motion associated with this wave should be focused in the area directly downstream, across the Dakotas and Minnesota. Therefore, it is unlikely that this contributed significantly to the severe weather later in the day.

However, as the day went on, a feature that was quite subtle on the 12Z 300 mb chart became more evident. At 12Z, a strong 90 m/s (175 knot) jet streak is embedded in the broader northwesterly flow over Oregon and northern California, with only subtle curvature in the geopotential height lines in that area. By early afternoon, however, this feature became quite evident on water vapor imagery (Fig. 4), as it developed into a separate wave with a more distinct circulation. This fast-moving feature continued to dig to the south and was able to reach Colorado and New Mexico by 00Z, by that time exhibiting more significant curvature in geopotential height lines at 300 mb. This turned out to be just in time to provide synoptic lifting for the convection just beginning to develop in Oklahoma and Texas, downstream of the wave. In addition to providing lift, the arrival of this wave also served to increase bulk shear over Oklahoma and Texas, with 300 mb flow increasing from around 30 m/s (60 knots) to over 50 m/s (100 knots) by 00Z.

The combination of these various synoptic processes effectively set the stage for the development of severe weather late in the day. To summarize, a synoptic cold front supported storms which reinforced a more subtle boundary in Oklahoma, providing a focal point for convective initiation later in the day. The combination of advection of warm air at 850 mb and the EML above by southwesterly flow across Texas with very moist air below the inversion resulted in a convectively unstable air mass across Texas

and Oklahoma. Finally, the arrival of an upper trough by early evening provided the large scale lift necessary to help erode the capping inversion and allow deep convection to develop, in addition to enhancing bulk shear by increasing upper level flow.

Despite the presence of these synoptic features, it is important to contrast this pattern with far more dynamically forced situations. While the broad upper trough over the western United States and arrival of the wave over Colorado and New Mexico provided a generally supportive environment, in a classic outbreak situation one would expect a deeper trough with a strong jet streak near its base crossing the Rockies, as well as strong southwesterly flow across much of the Plains downstream of the approaching trough. Instead, the large-scale support was more subtle and it is likely that this lack of overwhelming synoptic forcing was a primary limiting factor for this event. Consequently, rather than widespread convective initiation across many states, the result in this case was two smaller areas of initiation in the Texas panhandle and eastern Oklahoma. Clearly synoptic arguments do little to explain this distribution of storms. Instead, one must turn to the mesoscale; in this case, a detailed inspection of surface boundaries and other mesoscale features do as much to explain the distribution and timing of convection as synoptic arguments.

IV. Mesoscale Analysis

In order to analyze the mesoscale details of this event, first a detailed radar analysis of the two areas of interest will be conducted in order to provide more concrete evidence for the two distinct storm modes. Next, a description of the evolution of the surface boundaries will be given to explain the observed distribution of storms and the important mechanisms for their initiation. Finally, observed soundings, WRF model soundings, and other data from the WRF output will be combined with a conceptual model to investigate the reasons for the two distinct storm modes and different types of severe weather produced in each area.

In the Texas panhandle, the first significant storm became evident on radar in Crosby County at 23Z. This lone storm

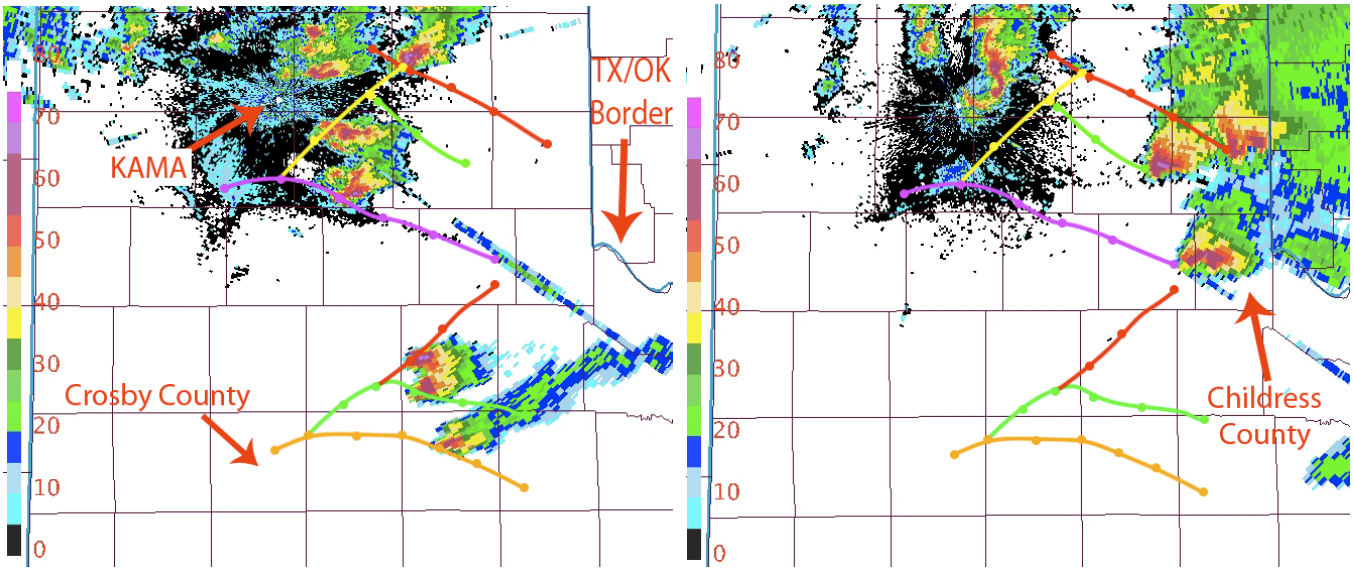

Fig. 5: Base reflectivity images from Amarillo, TX (KAMA) radar at 00:18Z (left) and 02:07Z (right) on May 10, 2006. Subjective storm tracks are drawn to demonstrate the movement of individual storm cells.

quickly split into a right-mover and left-mover, and by 0:30Z the left-mover had split again, forming three discrete cells across an area of 60 km (Fig. 5). At this time the middle cell produced a 70 dBz echo, which through storm reports appears to be correlated with 2" hail. About 40 minutes later, all three cells weakened quickly, with the middle cell dissipating first and the northern and southern cells dissipating shortly thereafter. The time from the formation of the first cell to the dissipation of the three resulting cells was about two hours.

Although these storms formed in an area far enough from surrounding radar sites to conduct a proper analysis of radar velocity data, the splitting character of these storms allows one to confidently classify them as supercells. This will be discussed in more detail later in this section. This radar data and the observed storm reports also provide good evidence for further classification of this group of storms as low-precipitation (LP) supercells, based on their small and concentric radar reflectivity structure as well as that they favor large hail production over other forms of severe weather (Bluestein and Woodall 1990).

Further to the north, more prolific storms in terms of their severe weather production formed around a similar time as the LP supercells to the south. Prior to initiation, weaker multicellular convection moved in south of the northern Texas border and produced an outflow boundary visible as a fine-line on radar (this is to the north of the visible area in Fig. 5). By 0:20Z about four distinct cells were evident to the south of this outflow boundary. The cell that is initially just to the southeast of the radar site moved on a trajectory similar to that of the left-movers in the group of LP cells to the south, while the rest moved on a right-mover trajectory. This left-mover underwent a collision with the storm initially just to the northeast of the radar site, and the remaining two cells began to exhibit a classic supercellular radar appearance. By 2Z three discrete supercells are present in the extreme eastern portion of the Texas panhandle, the northernmost of which had briefly produced a clear hook echo around 1:20Z and then produced a 75 dBz echo shortly thereafter. The furthest south of the three produced several 2"+ plus hail reports before becoming tornadic around 2:30Z as it moved through

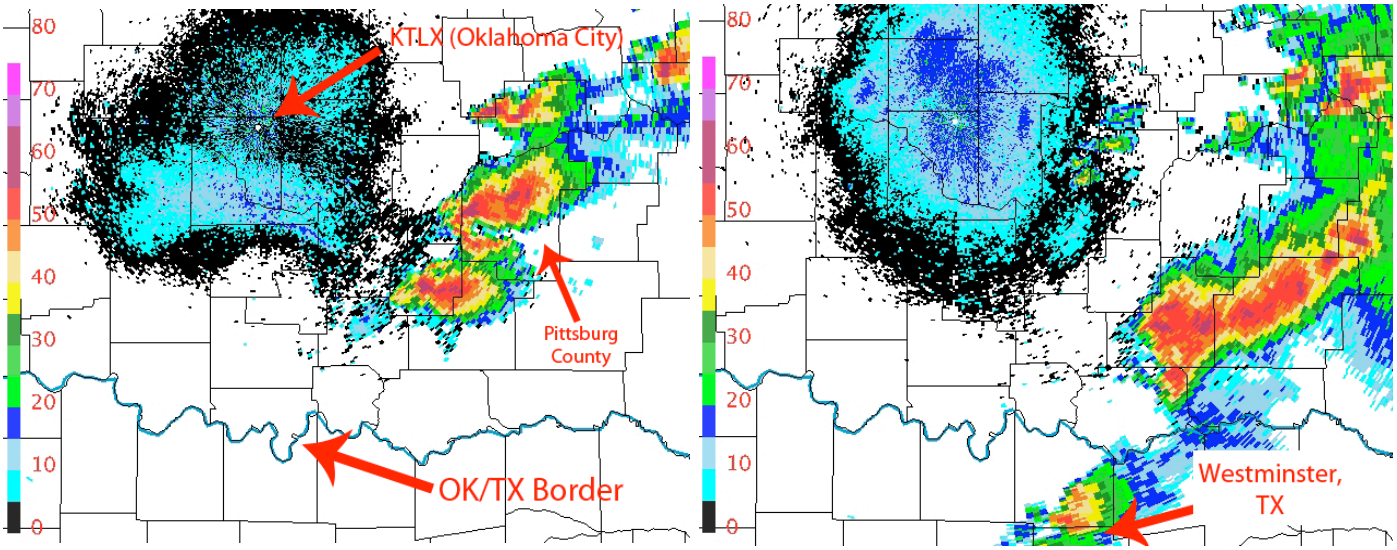

Fig. 6: Base reflectivity images from Oklahoma, OK (KTLX) radar at 00:06Z (left) and 02:00Z (right) on May 10, 2006.

the town of Childress**,** producing an F2 tornado on the eastern side of the city.

The discrete nature of these storms, the presence of hook echoes, and the presence of well-defined rotation couplets on velocity data from the same radar site (not depicted) again provide excellent evidence for the presence of well-developed mesocyclones in these storms. It is interesting to note that even within the Texas panhandle environment, where supercellular convection is the dominant storm mode in general, two distinct *types* of supercellular convection exist. In the storms to the south, left-movers are able to persist and the reflectivity structure is suggestive of an LP storm mode, while the storms to the north exhibit a classic supercellular structure with less clearly identifiable left-movers.

In the other area of interest, initiation occurred to the east and southeast of Oklahoma City, OK around 23Z. By the time these initial cells became established around 00Z, three discrete cells were present (Fig. 6). Throughout the next hour, the storm furthest to the south produced two brief tornadoes. Also around 00Z, the cell to its north produced the only large hail reports associated with this group of storms, with 2" hail reported in Pittsburg County.

However, these storms only remained discrete for a short period of time. By 1:30Z, the storms had congealed into a solid line spanning a distance of about 130 km. From this point on, the line of convection continued into Arkansas and produced only high wind reports. As mentioned previously, a single discrete cell can be seen in Fig. 6 south of the main line of storms. This is the deadly F3 producing storm that affected Westminster, Texas. However, it is over 200 km from the radar site so it is not well represented in this figure.

The evolution of this area of storms demonstrates well the importance of storm mode in determining the type of severe weather produced. The storms to the southeast of Oklahoma City produce primarily large hail and some tornadic activity for as long as they remain discrete, and then begin producing primarily damaging winds after congealing into a line. At the same time this line is producing severe wind, the discrete cell to its south is producing a significant tornado.

A detailed analysis of surface observations from around the time of initiation provides excellent insight into the resulting distribution of storms (Fig. 7). At 23Z a surface low is analyzed in north central Texas, with a lowest observed surface pressure of 999 mb. This low had deepened since the 18Z surface observations, at which point the lowest observed pressure was 1002 mb.

As Fig. 7 shows, a complicated situation had evolved and various boundaries stretching out from the surface low can be analyzed. While there was little in the way of temperature contrast across central Texas, observations from earlier in the afternoon (not shown) provided good evidence for a cold front to the northwest of the position analyzed in this figure, and the continued presence of the front is suggested by west-northwesterly wind observations to the southwest of the surface low. It appears this cold front had begun to overrun a dryline that had become caught up in the circulation of the surface low and mixed eastward into central Texas. The air mass to the north of the analyzed location of the cold front was still relatively moist, with dewpoints in the low to mid-40's (F); stations to the west of the analyzed dryline were reporting dewpoints of 20F and below; finally, 70F and higher dewpoints were

present to the east of the dryline. This suggests the presence of three distinct air masses in the area. Although they will not be explored further in this paper, large hail producing storms had also formed along this dryline in south central and extreme southern Texas.

To the northwest of the surface low is the first area of interest. Surface observations from this region suggest a post-frontal air mass as described above, with dewpoints through most of the northern portion of the panhandle in the upper-40's (F). Recall that weaker convection was moving into the extreme northern panhandle around this time. This is evident in the surface observations with the station in the extreme northwestern portion of the panhandle reporting 25 knot northwest winds, and a temperature of 63F, cooler than surrounding stations.

At first glance, this area does not appear particularly supportive of severe convection, with the highest dewpoints in the lower-50's (F) and a lack of any obvious surface boundaries. However, the most telling parameter here appears to be surface dewpoints. In eastern New Mexico, weak southwesterly winds and dewpoints in the 20's-30's (F) suggest the development of dryline circulation distinct from the one in central Texas. Dewpoint contours reveal a strong north-south moisture gradient generally parallel to the observed north-south line of convective development occurring at the same time. In addition, a moist tongue can be seen wrapping around into the

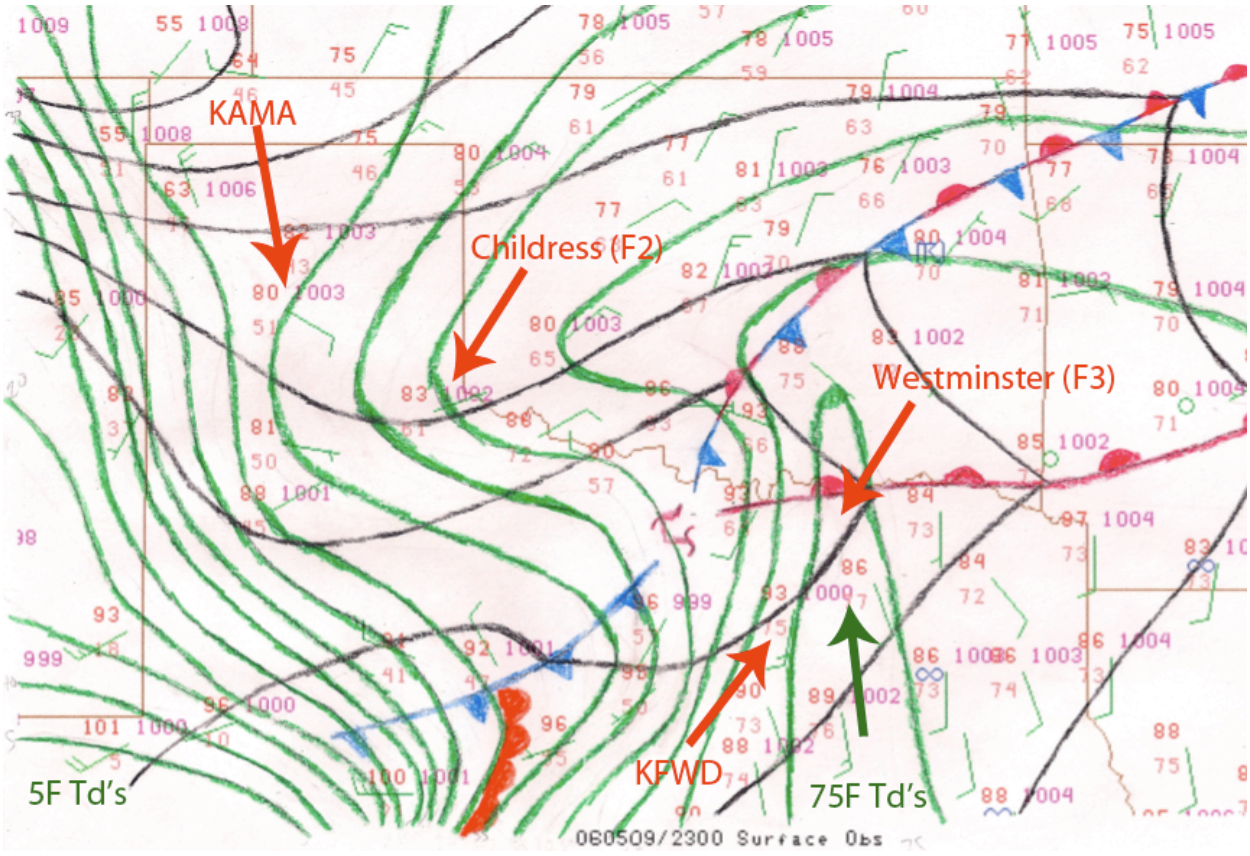

Fig. 7: Subjective surface analysis at 23Z on May 9, 2006 showing surface fronts, dewpoint contours every 5˚F (green), and isobars every 2 mb (black). Various locations referenced in the text are also marked.

northwest quadrant of the surface low, enhancing surface dewpoints just to the south of the panhandle. Note in particular that the axis of this moist tongue runs directly through Childress, Texas, where one cell produced an F2 tornado three hours after the current surface analysis. It is likely that this cell was bringing slightly elevated parcels into its updraft during the first hours of its life cycle, as it formed above relatively weak surface dewpoints. Later, as it moved to the southeast and encountered the greater surface moisture associated with this moist tongue, it was able to become surface based, lowering the Lifted Condensation Level (LCL) of lifted parcels. Thompson et al. 2002 provides strong statistical evidence that lower LCL heights are favorable for tornadogenesis, helping to explain the timing of this storm's tornado production.

This moisture analysis does an excellent job of explaining the behavior of storms in this area. After initiating along the subtle dryline circulation described above, the LP storms seen previously on radar formed on the southern fringe of the moisture tongue, and the rightward movement of two of the three cells brought them away from the richest moisture, explaining their quick demise. The supercells further to the north also formed along this dryline but these storms were instead able to strengthen because they moved to the southeast towards the region of better low-level moisture.

The second area of interest is in the northeast quadrant of the surface low. Note the entire area to the east of the low is in a region of rich low-level moisture, with dewpoints generally above 70F and a small tongue of enhanced 75F+ dewpoints to the southeast of the low.

The frontal feature stretching out to the northeast of the surface low is suggested primarily by a wind shift across this boundary. The convergence of surface wind along this zone corresponds quite well to the location of convective initiation in this area, especially in the area directly east of Oklahoma City. This focus of low-level convergence is likely what provided the extra lift necessary to erode the cap and initiate storms in this area.

The location of surface boundaries also provides some insight into the tornadic cell that moved through Westminster, Texas later in the evening. In addition to being located on the northern tip of the tongue of 75F+ dewpoints, later surface observations depict the surface low continuing a slow eastward drift in the hours following the 23Z analysis. This places the low of the surface low just to the west of Westminster, and the enhanced cyclonic circulation to the east of the low would have led to backing surface winds, locally increasing low-level helicity and making tornadogenesis more likely.

Two observed upper-air soundings will now be analyzed in order to build a better three-dimensional picture of the atmosphere in the two areas of interest. As expected, due to the coarse time and spatial resolution of upper-air observations, it is difficult to find perfectly representative soundings for the two cases of interest. However, the above surface analysis provides good context to make apparent potential deficiencies in the following soundings due to their less than ideal locations. In addition, model soundings from WRF output will be examined later to further refine the picture of the near-storm environments.

Nevertheless, two reasonably representative soundings were found. The first is from 00Z at Amarillo, Texas (KAMA, Fig. 8). As mentioned previously, this area is dominated by a post-frontal air mass with

surface dewpoints around 50F; this is quite dry compared to the 70F dewpoints in eastern Oklahoma. However, thanks to nearly dry-adiabatic lapse rates from the surface to about 600 mb, the sounding still exhibits sufficient convective instability for severe weather, with a surface-based CAPE of around 1300 J/kg.

The 00Z KAMA surface observation reports thunder, which makes this sounding less than ideal, as convection is already ongoing. This convective contamination is evident in the sounding, with a completely uncapped temperature profile and near-saturation from 700-500 mb. The shear profile, however, provides some evidence for the behavior of the storms in the area. Backed, southeasterly surface winds below westerly 55 knot flow at 6 km result in a 0-6 km bulk shear value of 61 knots, which is sufficient to support rotating storms (Thompson et al. 2002). In addition, the lowest three kilometers provide a good clue as to why cyclonically rotating, right moving storms were favored in the area around this sounding. Southeasterly surface winds smoothly veering to west-southwesterly at 3 km result in a curved hodograph with an adequate 0-3 km storm relative helicity of 194 m^2/s^2. More on the physical role of this shearing profile in creating rotating supercells will be presented later in this section.

The most representative 00Z sounding for the group of storms in eastern Oklahoma is from Fort Worth, Texas (KFWD, Fig. 9). Despite being 200 km from the nearest convection, based on surface observations it appears to be located in a similar air mass, compared to the nearer sounding site of Oklahoma City to the west, which is located in a cooler and drier air mass with northeasterly winds.

In the KFWD sounding, steep lapse rates are observed through the entire troposphere with dry adiabatic lapse rates from the surface to almost 500 mb, and only a very shallow stable layer at 700 mb. This

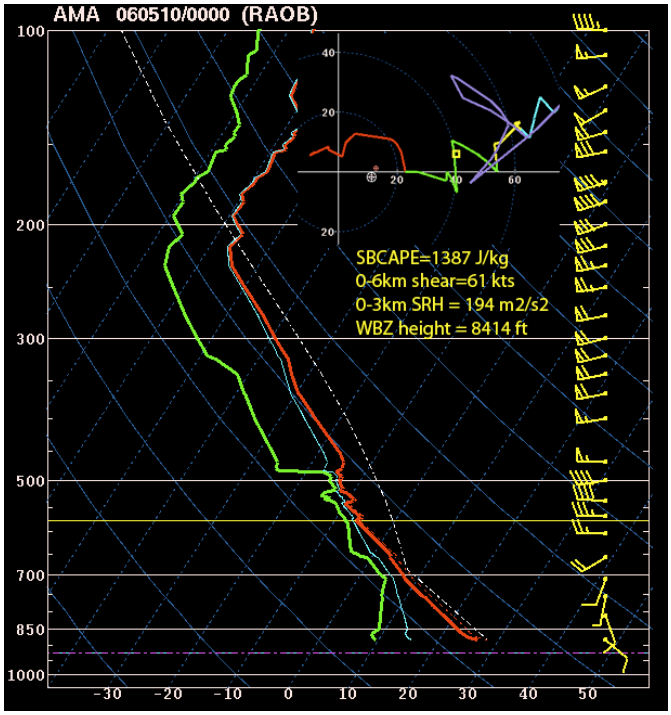

Fig. 8: Skew-T and hodograph from Amarillo, TX (KAMA) at 00Z on May 10, 2006. For the hodograph, 0-3 km is in red, 3-6 km is green, 6-9 km is yellow, 9-12 km is blue, and 12-15 km is purple.

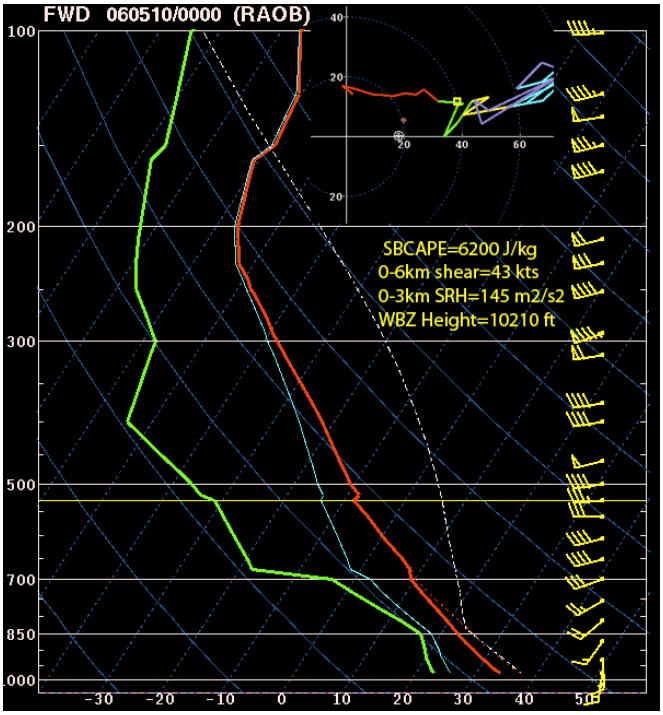

Fig. 9: Same as Fig. 8 but for Fort Worth, Texas (KFWD).

combined with a surface temperature/ dewpoint reading of 91/74F result in an extreme surface-based CAPE value of over 6000 J/kg in a nearly uncapped environment. Yet storms do not initiate as far south as KFWD, demonstrating the need for some kind of low-level convergence boundary or forcing mechanism for storm initiation even in a region of extreme CAPE and weak inhibition.

The extreme CAPE in this region is particularly interesting because it might lead one to expect very large hail formation in any storms that can form, due to strong, very buoyant updrafts able to support large hailstones. Yet the storms in southern Oklahoma, forming in a region of similarly extreme CAPE, only briefly produce large hail, while storms in the Texas panhandle forming in an environment of only about 1000 J/kg CAPE are able to consistently produce 2" or larger hail. This again suggests the possibility that convective mode does as much to influence the type of severe weather produced as a single parameter like CAPE, though clearly there are other factors important to hail production; for example, the wet-bulb zero height is in a more favorable range in the KAMA sounding (8414 ft) than the KFWD sounding (10210 ft) (Moore and Pino 1990).

The shear profile in the KFWD sounding is also quite distinct from KAMA. 0-6 km bulk shear is weaker than the KFWD sounding at 43 knots, due to slightly weaker 6 km winds and southerly instead of southeasterly surface winds. The preceding surface analysis depicts weak southeasterly surface winds near the storms in Oklahoma, which is quite different from the 15 knot southerly winds at KFWD. Therefore, reading too much into the low-level shear profile is probably not worthwhile, though it is noted that the straight-line 0-3 km hodograph at KFWD results in a smaller storm relative helicity of 145 m^2/s^2. Regardless, these subtle differences in shear profiles between the KFWD and KAMA soundings do the most to explain differences in storm mode between the two environments.

These differences in storm behavior caused by differing vertical shear profiles can

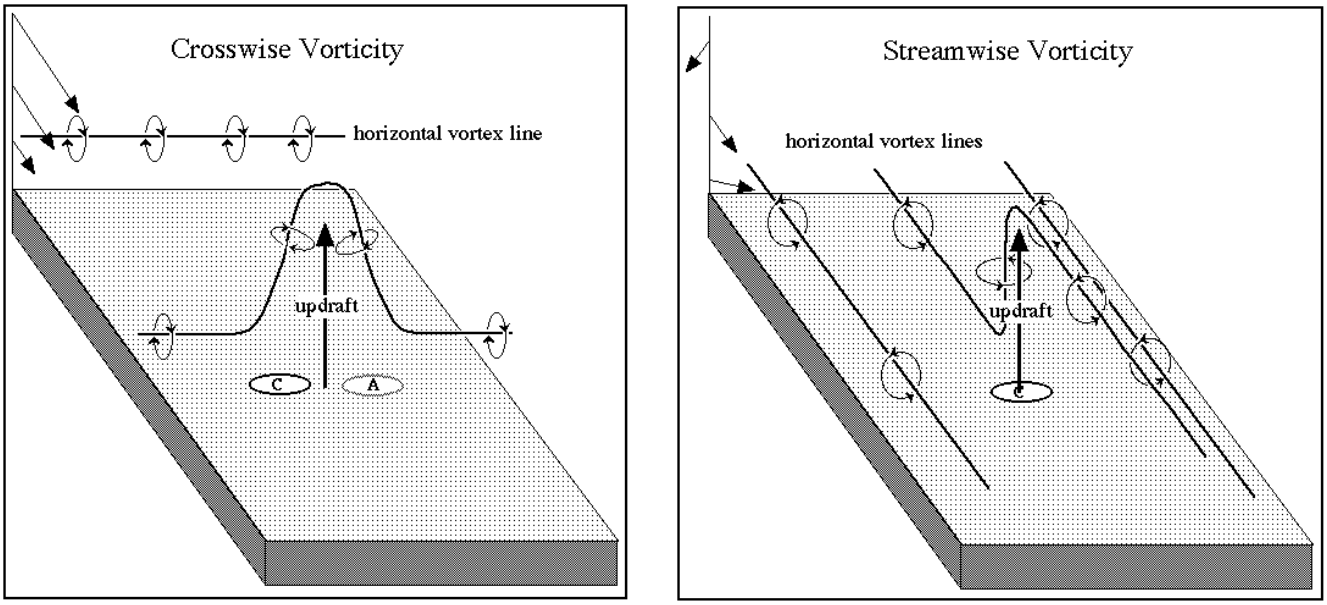

Fig. 10: Conceptual model illustrating the difference between crosswise (a) and streamwise (b) vorticity. Courtesy of Charles A. Doswell III, located at http://www.cimms.ou.edu/~doswell/vorticity/vorticity_primer.html.

be explained conceptually with a few simple yet powerful physical arguments. Based on the KAMA and KFWD soundings, the storms in Texas that exhibited greater supercellular behavior than those in Oklahoma formed in an area of both greater bulk shear and greater low-level helicity. In order to examine the role of these differences in shear, it is important to first distinguish between two separate types of shear.

The first is *crosswise vorticity* (Fig. 10a). The simplest case of crosswise vorticity is created by a vertical wind profile that increases in speed with height, but does not change direction. If one places an imaginary pinwheel in this flow, its rotation vector will point in a direction perpendicular to the flow itself. In itself this is not particularly important, but when one considers the role of a thunderstorm updraft superimposed on this environment, interesting things happen. The updraft actually tilts the vorticity, and due to its orientation with respect to the flow, vortices of a different sign are created. In other words, the left side of the updraft develops an anticyclonic rotation, while the right side develops a cyclonic rotation.

The second type of shear is streamwise vorticity (Figure 10b). The simplest case of this is a vertical wind profile that only changes in direction with height but remains at a constant speed. If one again imagines a pinwheel placed in this flow, its rotation vector will now be oriented parallel to the mean flow. Again, something interesting happens when an updraft superimposed on this environment is imagined. This time the updraft *only* rotates cyclonically; no anticyclonic couplet is present. Note that the updraft rotates cyclonically in this case because the shear profile in the diagram veers with height, as is commonly the case on severe weather days in the northern hemisphere. In a situation where the wind is backing with height, anticyclonic rotation would result.

In the real world, the best way to analyze the type of vorticity present in a given environment is the hodograph. It is clear that the simple crosswise vorticity case of unidirectional flow increasing with height would result in a straight-line hodograph, but a more general statement is that any flow resulting in a straight-line hodograph contains only crosswise vorticity. Similarly, while the simple case for streamwise vorticity results in a circular hodograph, any flow resulting in a curved hodograph contains streamwise vorticity. This can be seen readily in the hodographs of Figs. 8 and 9, where the KAMA hodograph exhibits curvature in the lowest three kilometers, in contrast to the KFWD hodograph which is almost a straight line in the lowest three kilometers; therefore, the KAMA hodograph has greater low-level streamwise vorticity.

In addition the visual inspection of hodographs, the helicity parameter is useful because it can be thought of as a measure of streamwise vorticity. Helicity is defined as the dot product of the vorticity and wind vectors, which is then integrated through some vertical portion of the sounding, generally 0-3 km. If one carefully considers the type of wind profile required to maximize helicity, it is clear that a circle hodograph is the result. Therefore, environments of large helicity are also environments where streamwise vorticity dominates over crosswise vorticity.

Putting all these pieces together has important implications for the behavior of storms. In environments of primarily crosswise vorticity, one would expect splitting supercells where the anticyclonic left-mover and cyclonic right-mover are

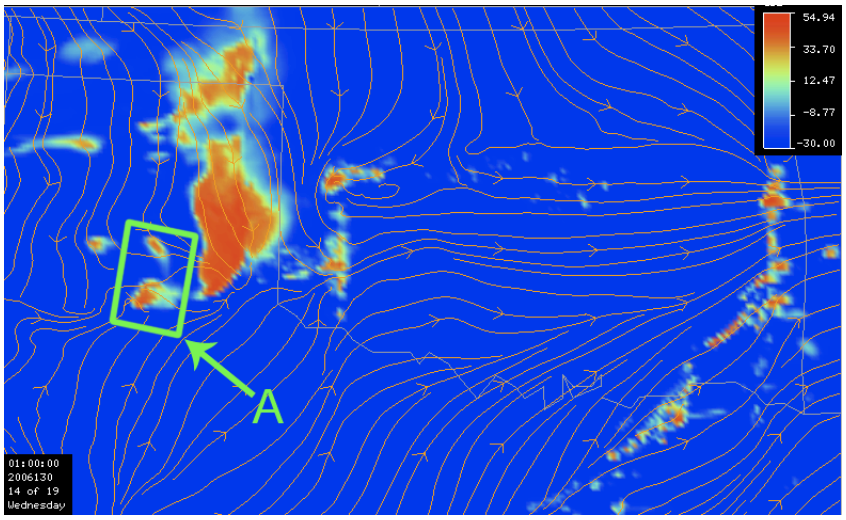

Fig. 11: WRF-simulated radar reflectivity (dBz, color fill) and horizontal streamlines, both at 2.1 km at 1Z on May 10, 2006. "A" marks the location of the right and left movers referenced in the text.

favored equally. In environments of streamwise vorticity, given a veering wind profile with height, one would expect the cyclonic right-mover to persist and the anticyclonic left-mover to either not form or dissipate quickly. In the case of the Texas panhandle storms, this immediately leads to the hypothesis that the northern storms, where primarily right-movers are present, formed in an environment of greater streamwise vorticity than the storms to the south, where both left-movers and right-movers can be clearly seen. Of course, a higher-resolution upper-air network would be required to confirm this observationally.

The larger helicity and bulk shear in the KAMA sounding than the KFWD sounding helps to explain the supercellular behavior of the Texas panhandle storms. However, based on this conceptual model, the straight-line KFWD hodograph should result in splitting supercells favoring both left and right-movers. Yet instead of splitting supercells the eventual result in eastern Oklahoma was a congealed line with little rotation. This shows that while distinguishing between streamwise and crosswise vorticity is helpful *if* the dominant storm mode turns out to be discrete supercells, it does not do as much to explain the difference between supercells and other storm modes. In reality, other factors were likely at play that kept the Oklahoma storms from being able to remain discrete and from forming mesocyclones. The most likely culprit is insufficient bulk shear given the extreme CAPE values in the area. Recall that the KFWD sounding contained 41 knots of 0-6 km bulk shear. However, surface winds further north were weaker, therefore lowering bulk shear even further in the actual storm environment. This hypothesis is supported by Thompson et al. 2002, which shows that supercell characteristics become marginal as 0-6 km shear is reduced to below 40 knots.

Lastly, the output of the WRF model run will be examined to determine if its high resolution output can provide any additional insight into the hypotheses proposed thus far. The results (Fig. 11) from over the Texas panhandle are considered first. Most exciting is the appearance of a small, splitting cell in the southern Texas panhandle, which by the time of Fig. 11 is evident as two separate cells (marked as "A" in the figure). These storms had begun as a single cell in the far southwestern panhandle and then split into the two cells that are present at 1Z. However, the simulation captures little of the detail of the storms in the central and northern Texas panhandle. Instead of relatively discrete supercells, the model produces a much more conglomerated group of storms. This feature had evolved out of the convection moving into the northern Texas panhandle rather than

forming separately as was seen in the actual radar data.

In eastern Oklahoma, the model has difficulty with initiating convection. The cells that have formed parallel to the Oklahoma-Arkansas border appear to be due to domain boundary effects, as their location corresponds well to the eastern border of one of the 2 km resolution domains. Along a line to the southwest of this feature storms that appear to have a more physical basis do form by 1Z. Despite their thin, somewhat unnatural appearance in the horizontal radar reflectivity slice, these cells do extend through the depth of the troposphere, with a mass of anvil spreading out around 13 km.

As already mentioned, the WRF run did produce one feature accurately: a splitting cell in the southern Texas panhandle. This allows for the investigation of one hypothesis considered previously. The 00Z KAMA observed sounding exhibited significant 0-3 km helicity in a region where radar data clearly showed right-moving supercells to be favored. This lead to the suspicion that the hodograph would become more of a straight line in the southern panhandle, where splitting cells were favored. The WRF simulation does provides some evidence to support this. A model sounding taken at 22Z from where the model-simulated splitting cell initially formed in the southwest Texas panhandle depicts almost straight westerly shear in the lowest 0-5 km of the atmosphere (Fig. 12). This results in a small 0-3 km storm relative helicity, which combined with a sufficient 51 knots of 0-6 km bulk shear makes the conceptual model consistent with the splitting storm produced by the WRF model.

On one hand, the difficulty the WRF model has with realistically simulating this event is a warning about putting too much trust into numerical model output in forecast

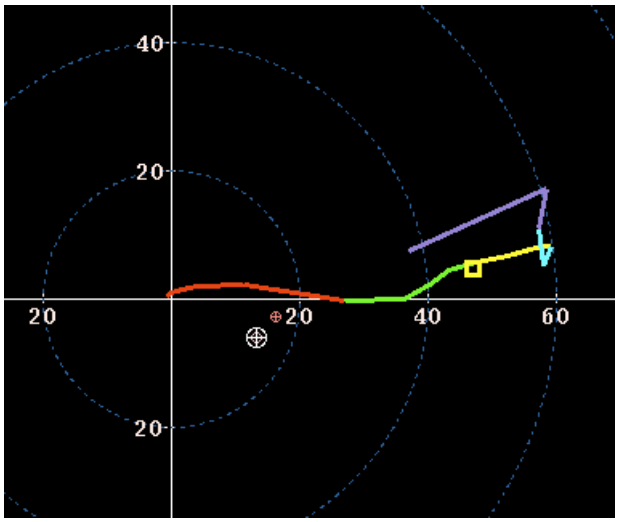

Fig. 12: WRF model hodograph from southwest Texas panhandle at 22Z on May 9, 2006. Colors are the same as Figs. 8 and 9.

situations, even as resolutions become high enough to simulate convection explicitly. On the other hand, these results are also a testament to the difficulty of the forecast problem that mesoscale dominated events like this one present. This difficulty is reflected in SPC convective outlooks through the course of the day; the 13Z outlook considered the most likely scenario for widespread severe weather to be the evolution of convection in the western Texas panhandle into a larger scale convective complex that would affect eastern Oklahoma and Arkansas overnight, rather than the two separate areas of afternoon development that actually occurred. This initial expectation led forecasters to issue a "moderate" risk for severe weather in this outlook. However, the 1630Z outlook downgraded the severe risk to "slight" as this scenario began to appear less likely.

V. Conclusion

The severe weather event of May 9, 2006 has been examined from a variety of perspectives and data sources. First, an overview of the large-scale situation was

presented, which demonstrated how the morning synoptic setup was able to create an environment conducive to convection later in the day. A subtle wave over northern California in the morning became more distinct through the day as it moved quickly eastward and finally helped to initiate convection late in the afternoon. Despite this feature, large-scale lift in general remained fairly weak; this observation combined with a strong capping inversion at 850 mb resulted in only limited convective development despite extreme CAPE values across eastern Oklahoma and northern Texas.

A detailed radar analysis was then conducted for each area of interest. The Texas panhandle storms were found to be quite distinct from those in eastern Oklahoma, and even within the group of storms in Texas significant differences were found, with right-moving classic supercells favored in the north and splitting LP supercells favored to the south. It was consistently shown that in general any storms that were able to remain discrete produced primarily large hail while the linear storms in Oklahoma produced primarily high wind. In addition, the two significant tornadoes were both produced by discrete supercells. These observations emphasize the importance in correctly predicting storm mode if an accurate forecast of severe weather type is desired.

Next, a detailed surface analysis at the time of convective initiation was performed. This provided great insight into both the location and behavior of each group of storms. A low-level moisture tongue wrapping into the northwest quadrant of a surface low in north-central Texas played a significant role in shaping the group of storms in Texas, with the LP cells weakening as they moved away from the enhanced moisture and the northern cells strengthening as they moved towards it. In Oklahoma, the location of initiation correlated well with a surface convergence boundary in that area.

Two observed upper-air soundings were analyzed to build a 3-dimensional picture of the environment of each group of storms. Limited bulk shear and low-level helicity in Oklahoma were likely the limiting factor for these storms, despite their formation in a region of extreme CAPE. The storms in Texas formed in an environment of greater bulk shear and helicity and therefore exhibited more sustained supercellular behavior, despite far lower CAPE values. In addition, by distinguishing between crosswise and streamwise vorticity a simple conceptual model was discussed in order to explain many of the differences between the diverse range of storms present across the Texas and Oklahoma on this day.

Finally, output from a high-resolution WRF simulation was examined. It was found to not be particularly skillful in reproducing the observed storms from this event. However, it did produce a splitting storm in the southern Texas panhandle which appeared similar to the observed storms in the same area. As a result, model soundings in close proximity to this storm were examined and did provide evidence to support the theory that the LP supercells in the southern Texas panhandle did in fact form in a region characterized by primarily crosswise vorticity.

Overall, convective mode was found to be particularly important in determining the type of severe weather. In addition, it was found that subtle differences in vertical shear profiles can have large effects on convective mode. Most importantly, the importance of proper diagnosis of mesoscale features in understanding the distribution and character of convection was made clear by each step of the analysis of this event.

VI. Acknowledgements

- Dan Henz for his help.
- Professor Greg Tripoli for lectures and lecture notes.
- Pete Pokrandt for help in obtaining data.

VII. References

Bluestein, H. B. and G. R. Woodall, 1990: Doppler-Radar Analysis of a Low-Precipitation Severe Storm. *Monthly Weather Review*, **118,** 1640-1664.

Dial, G.L., and J.P. Racy, 2004: Forecasting Short Term Convective Mode and Evolution for Severe Storms Initiated along Synoptic Boundaries. *Preprints*, 22nd Conf. Severe Local Storms, Hyannis MA. Accessed at http://www.spc.noaa.gov/publications on May 1, 2009.

Gallus, W. A., N. A. Snook, and E. V. Johnson, 2008: Spring and summer severe weather reports over the midwest as a function of convective mode: A preliminary study. *Weather and Forecasting*, **23,** 101-113.

Kain, J. S., S. J. Weiss, J. J. Levit, M. E. Baldwin, and D. R. Bright, 2006: Examination of convection-allowing configurations of the WRF model for the prediction of severe convective weather: The SPC/NSSL Spring Program 2004. *Weather and Forecasting*, **21,** 167-181.

Moore, J. T. and J. P. Pino, 1990: An Interactive method for estimating maximum hailstone size from forecast soundings. *Weather and Forecasting*, **5,** 508-525.

NWS Ft. Worth Storm Data 2006. Accessed at http://www.srh.noaa.gov/fwd/?n=2006sd on May 2, 2009.

NWS Lubbock Local Weather Events: 9 May 2006 Severe Thunderstorms and Tornado Event. Accessed at http://www.srh.noaa.gov/lub/?n=events-2006-20060509_storms_tor on May 2, 2009.

Skamarock, W.C., J.B. Klemp, J. Dudhia, D.O. Gill, D.M. Barker, W. Wang, and J.G. Powers, 2005: A description of the Advanced Research WRF Version 2. *NCAR Tech Notes-468+STR*. Accessed at http://www.mmm.ucar.edu/wrf/users/pub-doc.html on May 1, 2009.

Thompson, R. L., R. Edwards, J. A. Hart, and A. M. S. Ams, 2002: An assessment of supercell and tornado forecast parameters with RUC-2 model close proximity soundings. *21st Conference on Severe Local Storms*, San Antonio, Tx, Amer Meteorological Society, 595-598.

Weisman, M. L., C. Davis, W. Wang, K. W. Manning, and J. B. Klemp, 2008: Experiences with 0-36-h explicit convective forecasts with the WRF-ARW model. *Weather and Forecasting*, **23,** 407-437.